Journal of Integrative Neuroscience

J. Integr. Neurosci. **2026**; 25(2): 43410
https://doi.org/10.31083/JIN43410

Original Research

Therapeutic Potential of Nerve Growth Factor-Modified Hair Follicle Stem Cells Transplantation in a Rat Model of Alzheimer's Disease

Dan Yang[1], Lina Liu[2], Jin Fu[1,*]

[1]Department of Neurology, The Second Affiliated Hospital of Harbin Medical University, 150086 Harbin, Heilongjiang, China
[2]Department of Neurology, The Fourth Affiliated Hospital of Harbin Medical University, 150001 Harbin, Heilongjiang, China
*Correspondence: jinfu_123@126.com (Jin Fu)

Academic Editors: Hongmin Wang and Bettina Platt
Submitted: 10 June 2025 Revised: 15 October 2025 Accepted: 3 December 2025 Published: 11 February 2026

Abstract

Background: Alzheimer's disease (AD) is a degenerative condition affecting the central nervous system and is the primary cause of dementia. Current therapies for AD are ineffective. Although brain regeneration via stem cell transplantation has therapeutic potential, suitable sources are limited. Hair follicle stem cells (HFSCs) are multi-potent cells and can differentiate into mesodermal and ectodermal lineages, and proliferate for extended periods. Nerve growth factor (NGF) is a neurotrophin that is vital for neuronal development and survival, and the regulation of apoptosis in neurodegenerative disorders. However, using HFSCs to treat AD has not been extensively investigated. Herein, we evaluated the therapeutic effects of HFSCs and the synergistic effect of NGF and HFSCs on AD. **Methods**: A rat model of AD was established by intrahippocampal injection of amyloid β-protein 1–42 (Aβ1–42). After 14 days, HFSCs and HFSCs overexpressing NGF were injected into the hippocampus of AD rats for therapy. The cognitive function of the treated AD rats was tested using the Morris water maze test. Congo red staining, immunohistochemistry, and enzyme-linked immunosorbent assay (ELISA) were used to detect deposition, as well as soluble Aβ1–40 and Aβ1–42 levels. Additionally, western blotting was used to assess tau protein, the phosphoinositide-3 kinase (PI3K)/protein kinase B/glycogen synthase kinase-3β (Akt/GSK-3β) pathway, and the levels of synapse proteins. **Results**: HFSCs and HFSCs/NGF transplantation not only significantly reduced Aβ deposition but also inhibited GSK-3β activity and reduced tau protein hyperphosphorylation by stimulating the PI3K/Akt signaling pathway. Moreover, HFSC and HFSC/NGF transplantation led to significant overexpression of the synaptophysin (SYP) and postsynaptic density protein 95 (PSD95) in the hippocampus of AD rats. **Conclusions**: HFSCs and NGF-modified HFSCs may become a promising treatment option for AD.

Keywords: Alzheimer's disease; cognitive dysfunction; hair-follicle stem cells; nerve growth factor; PI3K-Akt pathway

1. Introduction

Alzheimer's disease (AD) is a degenerative neurological condition that worsens gradually over time. It is characterized by memory loss and cognitive decline and has rapidly emerged as one of the most expensive, fatal, and burdensome diseases [1]. According to Alzheimer's Disease International, the worldwide occurrence of dementia in 2016 was approximately 50 million, with AD accounting for 60%–80% of the cases [2]. The World Health Organization has predicted that the global number of individuals affected by dementia will increase to 139 million by 2050, from 55 million in 2019, due to the aging of the population [3,4]. The percentage of deaths attributable to AD in the United States is increasing, in contrast to declining overall mortality rates from stroke and cardiovascular diseases. AD was officially the 6th most prevalent cause of mortality in the U.S. in 2019 and the seventh most frequent cause of death in 2020 and 2021 [5].

AD is distinguished pathologically by senile plaques, which are clumps of amyloid β-protein (Aβ) peptides outside of cells, and neurofibrillary tangles (NFTs) comprising hyperphosphorylated tau proteins in neurons, which lead to progressive neurodegeneration [6]. Various types of Aβ cause cellular toxicity *in vivo* and *in vitro*. Mutated or hyperphosphorylated tau species are susceptible to aggregate formation and may be involved in neuronal dysfunction [7]. In addition to these hallmark features, AD is distinguished by widespread synaptic dysfunction and neuronal death, resulting in cognitive decline and eventual dementia. Chronic inflammation, neuronal damage, inhibition of neurogenesis, and oxidative stress are commonly observed in individuals with AD and contribute to disease progression [8]. The importance and connections of these phenomena are currently under intense investigation.

Before lecanemab was approved as a treatment, patients with AD had access to only two classes of medication: (a) cholinesterase inhibitors, including donepezil, rivastigmine, and galantamine, which are used to treat individuals with mild, moderate, and severe AD dementia [9]; and (b) memantine, which is a medication with two activities—it serves as a noncompetitive antagonist of N-methyl-D-aspartate receptors and as an agonist of dopamine. Memantine manifests in individuals with moderate to severe AD [10]. On 7 January 2023, lecanemab was granted rapid approval by the U.S Food and Drug Administration for AD management, marking a significant advancement in the

treatment of this disease [11]. Stem cell transplantation is one of the most cutting-edge and promising experimental treatments for AD. Stem cells replace cells and use various methods to control inflammatory or damaged environments [12–14]. Hair follicle stem cells (HFSCs) are thought to be an excellent cell type for the treatment of neurological illnesses. Mouse hair follicles harbor HFSCs that express the neural progenitor marker nestin rather than the keratin cytokeratin [15]. McKenzie *et al*. [16] demonstrated that HFSC transplantation contributes to myelin-sheath development in the sciatic nerve in mice that have a genetic myelin basic protein deficit. Moreover, HFSCs first migrate to the brain and then to the fore-head, where they give rise to various neural phenotypes, including immature neurons and well-differentiated astrocytes in rodents model [17–19]. However, additional investigations are necessary to clarify the functions and mechanisms of HFSCs in AD.

Nerve growth factor (NGF) is categorized as a neurotrophin. Rita Levi-Montalcini first discovered it in mouse sarcoma in the early 1980s [20]. The peripheral nervous system, immunological cells, sensory afferents, sympathetic-efferent-innervated peripheral nerves, and the central nervous system (CNS) all express NGF [21]. In the CNS, certain areas, such as the cortex and hippocampus, which are targeted by cholinergic neurons, have an elevated level of NGF expression [22]. NGF is vital for neuron development [23], survival [24], and the regulation of apoptosis in mammals, including humans [25]. NGF starts signaling by binding to two distinct cell-surface receptors [26]: tropomyosin receptor kinase A (TrkA) and p75 neurotrophin receptor (p75 NTR), which are lower-affinity receptors. TrkA-mediated pathways are key for the growth and metabolism of neurons [27]. When NGF binds to the TrkA receptor, its intrinsic tyrosine kinase activity catalyzes TrkA's autophosphorylation, which activates three pathways: phospholipase C-γ (PLC-γ), extracellular signal-regulated kinase, and phosphoinositide-3 kinase (PI3K) [28–31]. These pathways have all been involved in AD treatment.

This investigation assessed the potential therapeutic benefits of HFSCs and NGF-modified HFSCs, and explored the underlying mechanisms, in a rat model of AD, in order to help develop new approaches for improving AD treatment.

2. Materials and Methods

2.1 Isolation and Culture of HFSCs

Hair follicles were extracted by mechanical dissection after enzymatic digestion [15]. To isolate the hair follicles, hair-follicle pads of male Sprague-Dawley (SD) rats (21–26 g; purchased from the Animal Experiment Center of the Second Affiliated Hospital of Harbin Medical University) were dissected and digested with 0.1% collagenase (17018029, Gibco, Thermo Fisher Scientific, Waltham, MA, USA) in Dulbecco's modified Eagle's medium (DMEM) (11965092, Gibco, Thermo Fisher Scientific). The hair follicles were then carefully extracted from the pads and placed into 12-well tissue culture dishes (Beyotime, Shanghai, China) for cultivation. The hair follicles were cultivated in DMEM/F12 (11320033, Gibco, Thermo Fisher Scientific) medium with 1% penicillin and streptomycin (15140122, Gibco, Thermo Fisher Scientific) and 10% fetal bovine serum (0025, ScienCell Research Laboratories, Santiago, CA, USA) at 37 °C in a humidified conditions with 5% CO_2. Cell growth was monitored under a microscope, and half-medium alterations were conducted every 2–3 days. Primary cultures were first passaged after 14 days of cultivation, followed by subsequent passages every 3–5 days. Upon reaching 85–90% confluence, cells were dissociated via Accutase™ (A1110501, Gibco, Thermo Fisher Scientific), a neural stem-cell-specific cell dissociation reagent, during passage. The third-generation HFSCs were cultivated (3×10^4 cells/cm^2) in a six-well tissue-culture-plate medium. Each procedure was carried out in a sterile setting. In this study, third-generation HFSCs were used. All cell lines were authenticated via autosomal short tandem repeat (STR) profiling and confirmed negative for mycoplasma contamination.

2.2 Construction of NGF-Overexpressing Gene-Modified HFSCs

The lentivirus vector was PLJM1-EGFP-puro (FH1717, Fenghui Biological Company, Changsha, Hunan, China). The third passage of cultured HFSCs was co-cultured with either NGF-overexpressing lentivirus (Gene: Lv-Rat-*NGF*-OE, *NM_001277055*) or blank lentivirus at a multiplicity of infection of 80 for 72 h. Specifically, 16 µL of virus stock with a titer of 1×10^9 transducing units (TU)/mL was added per mL of culture medium. Transduced cells were selected with 2.0 µg/mL puromycin dihydrochloride (58582, Sigma-Aldrich, St. Louis, MO, USA) and utilized for following trials. The average transduction efficiency was assessed via a fluorescence microscope (Nikon Eclipse Ti2, Tokyo, Japan) and calculated as (number of EGFP-positive cells/total number of cells) $\times$ 100%, which was approximately 75%.

2.3 Flow Cytometry

We performed surface-marker detection of the cell line using flow cytometry. Single-cell suspensions of third-passage HFSCs (4-week *in vitro* culture) were prepared, counted, and aliquoted ($\geq 1 \times 10^5$ cells) into 1.5-mL EP tubes. After centrifugation (1000 rpm, 5 min) and supernatant elimination, resuspension of cells was conducted in 100 µL flow staining buffer (R32816, Yuanye Bio, Shanghai, China) and incubated with flow cytometry (FC) blocking reagent (101302, BioLegend, San Diego, CA, USA) (20 µL/tube) at room temperature for 30 min to reduce non-specific binding. Fluorochrome-conjugated primary antibodies were added at optimized concentrations

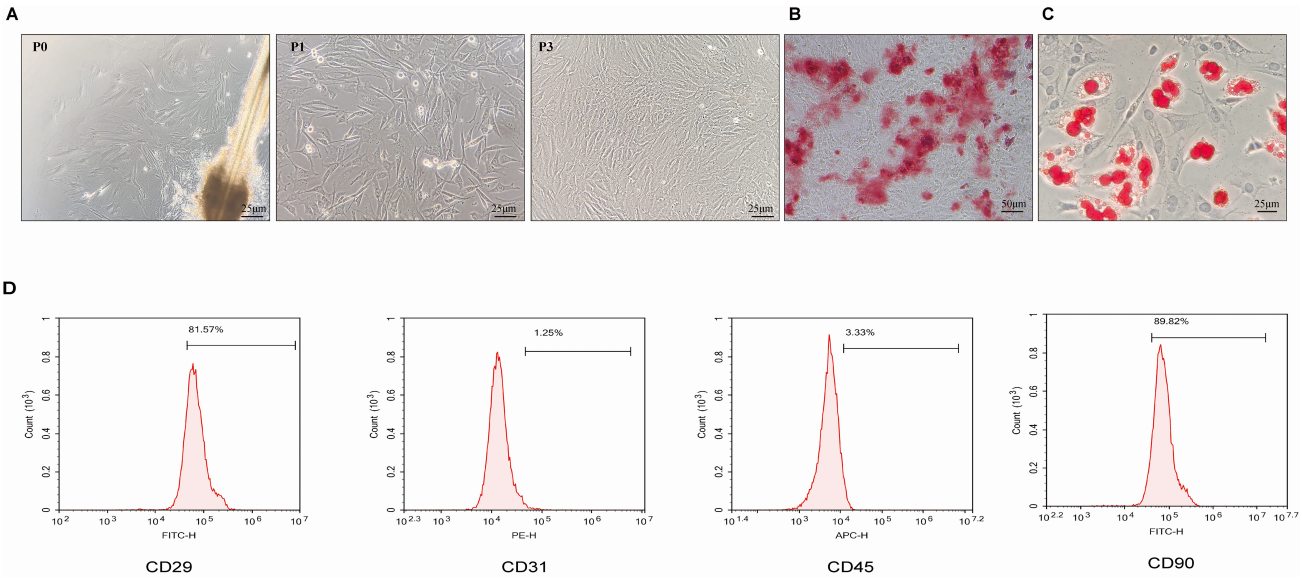

Fig. 1. Results of isolation, culture, and identification of HFSCs from the bulge region of hair follicles and the ability of HFSCs to poly-differentiate. Optical microscopy of an intact hair follicle, microdissected and extracted from the hair follicle in the bulge region for primary cell culture. (A) HFSCs in primary, P1, and P3 were under an optical microscope. After 14 days of culture, osteogenic and adipogenic differentiation was confirmed by (B) Alizarin red and (C) Oil Red O staining. (D) Flow cytometry detection of HFSCs surfaces positive markers CD29, CD90, negative markers CD31, CD45. (A,C) scale bar = 25 µm, (B) scale bar = 50 µm. Abbreviations: HFSCs, hair follicle stem cells; FITC-H, fluorescein isothiocyanate-height; PE-H, phycoerythrin-height; APC-H, allophycocyanin-height; CD, cluster of differentiation; P, passage.

(20 µL/1 × 10^6 cells): anti-rat cluster of differentiation 45-allophycocyanin (CD45-APC) (1:100, F3104503, Lianke Bio, Hangzhou, Zhejiang, China), CD31-PE (1:150, sc-18916 PE, Santa Cruz Biotechnology, Dallas, TX, USA), CD90.1 (1:100, HIS51, 14-0900-81, Thermo Fisher Scientific), and CD29-fluorescein isothiocyanate (FITC) (1:100, eBioHMb1-1, 11-0291-80, Thermo Fisher Scientific). An incubation of tubes was conducted in the dark at room temperature for 1 h, then washing was conducted twice with 1 mL pre-cooled flow-staining buffer (1000 rpm, 5 min centrifugation) to remove unbound antibodies. Cells were resuspended in 500 µL flow-staining buffer, protected from light, and analyzed on a BD FACS Canto II cytometer (BD Biosciences, San Jose, CA, USA) within 2–6 h. Isotype controls (detailed in the **Supplementary Material** "**Isotype controls.pdf**") were included to define background fluorescence. Gating excluded debris/aggregates via forward scatter (FSC) and side scatter (SSC) [FSC/SSC], with positive/negative populations distinguished using isotype control-derived fluorescence thresholds. Flow cytometry analysis showed that the cell surface markers CD29 (a well-recognized marker for HFSCs) and CD90 (cytokeratin) were highly expressed in our isolated HFSCs, and CD31 (a marker for vascular endothelial cells) and CD45 (a marker for hematopoietic cells) were expressed at low levels (Fig. 1D). These results are consistent with the identification criteria.

2.4 Osteogenic and Adipogenic Induction of Differentiation of HFSCs

As directed by the manufacturer [32], the growth medium was exchanged for an osteogenic or adipogenic differentiation medium after a 24-h incubation. Three days were given for a shift in the osteogenic and adipogenic differentiation media while the cells were cultivated in an appropriate environment at 37 °C with 5% CO_2. Alizarin red (Y027377, Beyotime) and Oil Red O (Y264669, Beyotime) were used to confirm osteogenic and adipogenic differentiation after 14 days of culture.

Flow cytometry was applied in order to detect cell-surface markers. The 3rd-generation HFSCs cell suspension was made by digesting the cells with trypsin (0.25%, 25200056, Thermo Fisher Scientific), then rinsing two times with phosphate buffered saline (PBS), and finally adjusting to 1 × 10^5 cells/mL. Afterward, the cells were incubated with an antibody against CD29 (0.5 mg/mL; 11-0291-82; Thermo Fisher Scientific) coupled with fluorescein isothiocyanate isoform, isophycocyanin conjugated antibody against CD90 (0.5 mg/mL; 14-0900-81; Thermo Fisher Scientific), phycoerythrin-conjugated antibody against CD31 (2 mg/mL; sc-18916; Santa Cruz Biotechnology), or phycoerythrin-conjugated antibody against CD45 (5 µL/test; F3104503; Multisciences, Hangzhou, Zhejiang, China) for 1 h at room temperature. Staining was stopped with 1% bovine serum albumin, after which loading the cells onto a flow cytometer

was conducted (NovoCyte Advanteon, ACEA Biosciences, California, CA, USA). The same procedure was used for isotype controls.

2.5 Animals

The Animal Experiment Center of the Second Affiliated Hospital of Harbin Medical University provided clean-grade, male, SD rats (6–8 weeks old, 200–210 g) [License No. SCXK (Hei) 2023-001]. All rat experiments were conducted as per the principles outlined in the "Guide for the Care and Use of Laboratory Animals" published by the Ministry of Science and Technology of the People's Republic of China. Sixty were randomly allocated into four groups (n = 15/gp): Sham+PBS, Aβ+PBS (AD+PBS), Aβ+HFSCs (AD+HFSCs), and Aβ+HFSCs/NGF (AD+HFSCs/NGF) groups (designated depending on the substance injected into the hippocampus). The experimental design for this hippocampus-targeted AD study was based on previous literature [33]. Experimental AD was established by stereotaxically injecting human Aβ1–42 (ab82795, Abcam, Cambridge, UK) diluted to 1 mg/mL, bilaterally, into the hippocampal cornu ammonis 1 (CA1) region (coordinates: A/P = +3.0 mm; M/L = +2.0 mm; D/V = +3.0 mm). Rats were anesthetized with 0.3% pentobarbital sodium (40 mg/kg, P3761, Shanghai Pharma, Shanghai, China) by i.p. injection and fixed in a stereotactic apparatus (RWD Life Sciences, Shenzhen, Guangdong, China). A microinjector (RWD Life Sciences) injected 10 µL Aβ1–42 solution into each side of the hippocampus (injection speed: 1 µL/min). In the Sham group, 10 µL of PBS was administered using the same method. After 14 days, rats were chosen randomly from Sham and Aβ groups to run in the Morris water maze test, then anesthetized with 0.3% pentobarbital sodium (150 mg/kg) i.p. for euthanasia and then exposed to Congo red (MS4060-25G, Maokang Biotechnology, Shanghai, China) staining (n = 3). The remaining rats in the Sham and Aβ groups were injected with 10 µL of PBS. Aβ+HFSCs and Aβ+HFSCs/NGF groups were subjected to 10 µL modified or unmodified HFSCs suspension (5×10^5 third-generation) through the same needle track as the Aβ1–42 injection. On day 29, all rats underwent Morris water maze training and testing. Six days later, the rats were euthanized under intraperitoneal anesthesia with 0.3% pentobarbital sodium (150 mg/kg) and rat brains were harvested for analysis.

2.6 Congo Red Staining

After being anesthetized, rats were subjected to transcardial perfusion with 0.9% physiological saline via thoracic cavity exposure. Brains were subsequently dissected, immersed in 4% paraformaldehyde (70-F0001; MultiSciences) for fixation, then PBS was utilized for rinsing. After that, the tissues were processed through gradient dehydration, paraffin-embedded, and sliced at a thickness of 40 µm. Then, slices were deparaffinized, followed by gradient rehydration and stained with Congo red dye for 10–20 min, then differentiated with alkaline ethanol differentiation solution for several seconds, and washed with water, then counterstained with hematoxylin (H3136; Sigma-Aldrich) for 2 min and rinsed with running water for 1–2 min. After that, the slices were dipped in ascending grades of ethanol. Finally, they were cleared with xylene (214736; Sigma-Aldrich) and sealed with neutral resin (G8590; Solarbio, Beijing, China). The slides were photographed under an optical microscope (ECLIPSE Ti2-U, Nikon).

2.7 Immunohistochemical Staining

The immersion of paraffin slices was conducted in 0.3% H_2O_2 for 30 min. Next, normal goat serum (c0265, Beyotime) was utilized to block the slices for 30 min at 25 °C, then an overnight incubation with primary mouse anti-β-Amyloid antibodies (6E10, 1:500 dilution; 803001, Biolegend) was conducted at 4 °C. The next day, they were rinsed 3 times with PBS, incubated at 37 °C for 1 h with the second antibody (1:500, ab205718, Abcam), and then washed with PBS. They were then visualized with a 3,3'-Diaminobenzidine (DAB) substrate kit (ab64238, Abcam). Sections were PBS-washed, counterstained with hematoxylin, and then hyalinized and dehydrated. An optical microscope was used to observe the staining effect and take photos.

2.8 Morris Water Maze Test

The rats underwent a navigation test in a water maze (the water temperature was controlled at 25 $\pm$ 1 °C) for 5 consecutive days. The experimental environment was strictly standardized: Four fixed visual cues (30 $\times$ 30 cm; red circle, blue square, yellow triangle, green bar) were placed on the maze walls. Room conditions (light intensity: 200 lux; noise level: $<$40 dB) and the experimenter's position were controlled to ensure reliable use of spatial cues by rats. The maze water was made opaque with 0.1% (w/v) food-grade titanium dioxide solution (Jianghu Titanium White Chemical Products Co., Shanghai, China) to hide the underwater platform. Prior to formal testing, all rats underwent habituation for 2 days before training: each was individually placed in the maze (without the platform) for 120 s of free swimming to become familiar with the pool, water temperature, and space. They were also adapted to the experimental room for 30 min daily to reduce environmental stress interference with behavior. For the 5-day navigation training, the rats were required to enter the water from four different quadrants with their heads facing the pool wall, and their movement trajectory and escape latency were recorded four times daily. Each training trial was limited to 60 s: if a rat reached the platform within 60 s, it was permitted to stay on the platform for 15 s to consolidate memory; if not, the experimenter guided it to the platform, where it stayed for 15 s. Escape latency is described as the time spent by the rat to first locate the underwater platform

after entering the water. The spatial-probe test was conducted on the sixth day after the start of the water maze training. Rats were set into the water from the quadrant opposite to the original location of the platform, after the platform was eliminated, and the count of platform crossings was recorded.

Behavioral testing and image quantification were conducted blindly. All animals were ear-tagged for identification. Group allocation was done by a different person; both the operators performing behavioral tests and the personnel collating data were unaware of the groupings, thus reducing bias.

2.9 Enzyme-Linked Immunosorbent Assay (ELISA)

Rats from every group were euthanized and the hippocampus was dissected for measurement of the protein levels of Aβ1–40 and Aβ1–42. This was achieved by using Aβ40 ELISA kits (ER0754, Wuhan Fine Biotech Company, Wuhan, Hubei, China) and Aβ42 ELISA kits (ER0755, Wuhan Fine Biotech Company), as per the manufacturer's guidelines. The quantified amounts of soluble Aβ, measured in picomolar units, were normalized to the total protein content of the cell lysate. The signal was identified via a Varioskan Flash multimode reader (Thermo Fisher Scientific).

2.10 Western Blotting (WB) Assay

The hippocampus was homogenized with a tissue extraction buffer that included protease inhibitors. This was accompanied by centrifugation at 12,000 rpm at a temperature of 4 °C for 10 min. The resulting supernatants were gathered and assessed for protein concentration with BCA protein assay kits (ab102536, Abcam). The protein samples, weighing 40 µg, were separated using 10% or 12.5% SDS-polyacrylamide gel electrophoresis (P0012A, Beyotime) at 100 V for 90–120 min. Then they were moved to a polyvinylidene fluoride (PVDF) membrane (88520, Thermo Fisher Scientific) using a current of 200 mA at 4 °C for 120 min. The PVDF membrane was preincubated with 3% nonfat milk in Tris-buffered saline with 0.1% Tween-20 (TBS-T) at 25 °C for 60 min to block nonspecific binding sites. The incubation of PVDF membranes was conducted overnight at 4 °C with primary antibodies targeting protein kinase B (Akt) (1:1000; 4685, Cell Signaling Technology, Danvers, MA, USA), phospho-Akt (Thr308) (1:1000; 13038, Cell Signaling Technology), glycogen synthase kinase (GSK)-3β (1:1000; 9315, Cell Signaling Technology), phospho-GSK-3β (ser9) (1:1000; 9336, Cell Signaling Technology), tau 5 (1:1000; ab80579, Abcam), p-tau (S396) (1:1000; CY5657, Abways, Shanghai, China), p-tau (S404) (1:1000; CY9003, Abways), p-tau (Thr231) (1:1000; CY6535, Abways), p-tau (Ser202/Thr205) (1:5000; 82568-1-RR, Proteintech, Rosemont, IL, USA), β-site amyloid precursor protein cleaving enzyme 1 (BACE1) (1:1000; CY6880, Abways), postsynaptic density protein 95 (PSD95) (1:1000; CY5407, Abways), synaptophysin (SYP) (1:1000; CY5273, Abways), PI3K (1:1000; 4292, Cell Signaling Technology), phosphorylated-PI3K (p-PI3K, 1:1000; 4228, Cell Signaling Technology) and loading control protein anti-β-Actin (1:3000; AF7018, Affinity, Changzhou, Jiangsu, China), anti-β-tubulin (1:1000; 2128, Cell Signaling Technology) and anti-glyceraldehyde-3-phosphate dehydrogenase (GAPDH) (1:1000; 2118, Cell Signaling Technology). After being rinsed 3 times with TBS-T, the PVDF membranes were incubated with secondary antibodies conjugated with horseradish peroxidase (P2369; Beyotime) and exposed to the enhanced chemiluminescence Plus Western Blotting Detection Kit (35050, Thermo Fisher Scientific). Three replications were performed. The immunoblot pictures were obtained via the Omega-Lum G imaging system (ChemiScope 6300, Clinx Science Instruments, Shanghai, China). Image-Pro 11.1 (Media Cybernetics, Inc., Rockville, MD, USA) was used to calculate bands for semi-quantification. All values were standardized based on an equal loading control.

2.11 Quantitative Real-Time Reverse Transcription PCR (qRT-PCR)

NGF levels in the untreated HFSCs, the HFSCs/Vector, and the HFSCs/NGF groups were quantified by qRT-PCR assay. In brief, total RNA isolation from the respective HFSCs was conducted via TriZol reagent (15596026CN, Invitrogen, Carlsbad, CA, USA). Reverse transcription was conducted via the PrimeScript RT reagent kit (RR037A, TaKaRa, Dalian, Shandong, China). Quantitative PCR was conducted via the SYBR PrimeScript RT-PCR Kit II (RR820A, Merck KGaA, Darmstadt, Germany) on an LC480 real-time PCR system (Influence Bio, Shanghai, China). The sequence of each primer is shown in Table 1.

Table 1. Target gene primer sequences for qRT-PCR.

Gene	Primer sequence
rat *NGF* F	ACTCTGTCCCTGAAGCCCACTG
rat *NGF* R	TGTTGCGGGTCTGCCCTGTC
rat *β-actin* F	GGAGATTACTGCCCTGGCTCCTAGC
rat *β-actin* R	GGCCGGACTCATCGTACTCCTGCTT

qRT-PCR, quantitative real-time reverse transcription PCR; NGF, nerve growth factor.

2.12 Statistical Analysis

Data are reported as the mean ± standard error of the mean (SEM). The density was measured via ImageJ software (Version 1.53t, Wayne Rasband, National Institutes of Health, Bethesda, MD, USA) . The statistical analysis and generation of statistical graphics were conducted using GraphPad Prism 9.5 software (GraphPad Software, LLC,

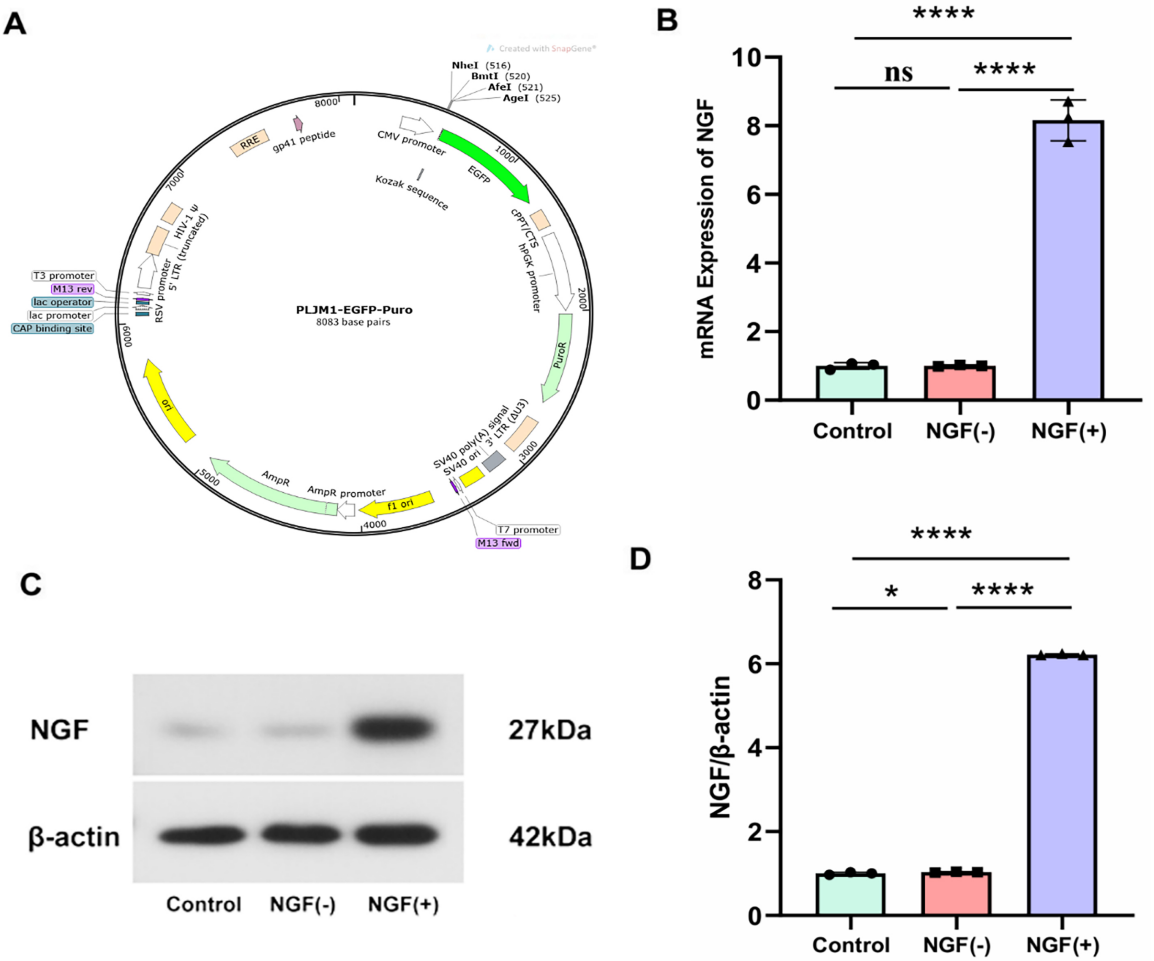

Fig. 2. Successful construction of NGF over-expressed HFSCs. (A) The structure of the lentivirus vector with NGF over-expressing. (B) The *NGF* mRNA level was quantified with Real-time PCR. (C,D) The NGF expression levels were estimated through western blot analysis. Data analysis was conducted by one-way ANOVA with Tukey's post-hoc test (B,D), *$p < 0.05$, ****$p < 0.0001$; ns, not significant, $n = 3$. Abbreviations: GAP, GTPase activating protein; RRE, rev response element; CMV, cytomegalovirus; EGFP, enhanced green fluorescent protein; CPPT, central polypurine tract; CTS, central termination sequence; hPGK, human phosphoglycerate kinase promoter; LTR, long terminal repeat; SV40, simian virus 40; *AmpR*, ampicillin resistance gene; RSV, rous sarcoma virus; HIV, human immunodeficiency virus; PLJMI-EGFP-*Puro*, PLJM1-enhanced green fluorescent protein-puromycin resistance gene.

San Diego, CA, USA). Data analysis was conducted with a 1-way analysis of variance and Tukey's test for several comparisons. $p \leq 0.05$ were deemed to be significant.

3. Results

3.1 Successful Isolation of HFSCs

HFSCs' isolation from the upper lips of male SD rats was conducted; hair-follicle pads were cultivated until the 3rd generation (Fig. 1A). After inducing the osteogenic differentiation, HFSCs differentiated into osteoblasts, confirmed by positive Alizarin red staining (Fig. 1B). Moreover, HFSCs differentiated into adipocytes, as manifested by the presence of lipid droplets with orange coloration upon staining with Oil Red O dye (Fig. 1C). These steps illustrated the multidirectional differentiation capability of HFSCs. Flow-cytometry analysis revealed that the cell surface markers of HFSCs, such as CD29 and CD90, were overexpressed, while the endothelial cell-surface marker CD31 and the hematopoietic cell-surface marker CD45 were suppressed (Fig. 1D).

3.2 Successful Construction of NGF Over-Expressed HFSCs

Fig. 2A illustrates the viral vector utilized in this investigation. The level of *NGF* mRNA expression was quantified by using PCR in the control, the HFSCs/Vector, and the HFSCs/NGF groups (Fig. 2B). The expression levels of NGF in these groups were assessed with WB analysis (Fig. 2C,D, the original WB images can be found in the **Supplementary Material**). These outcomes verified the HFSCs/NGF's successful construction.

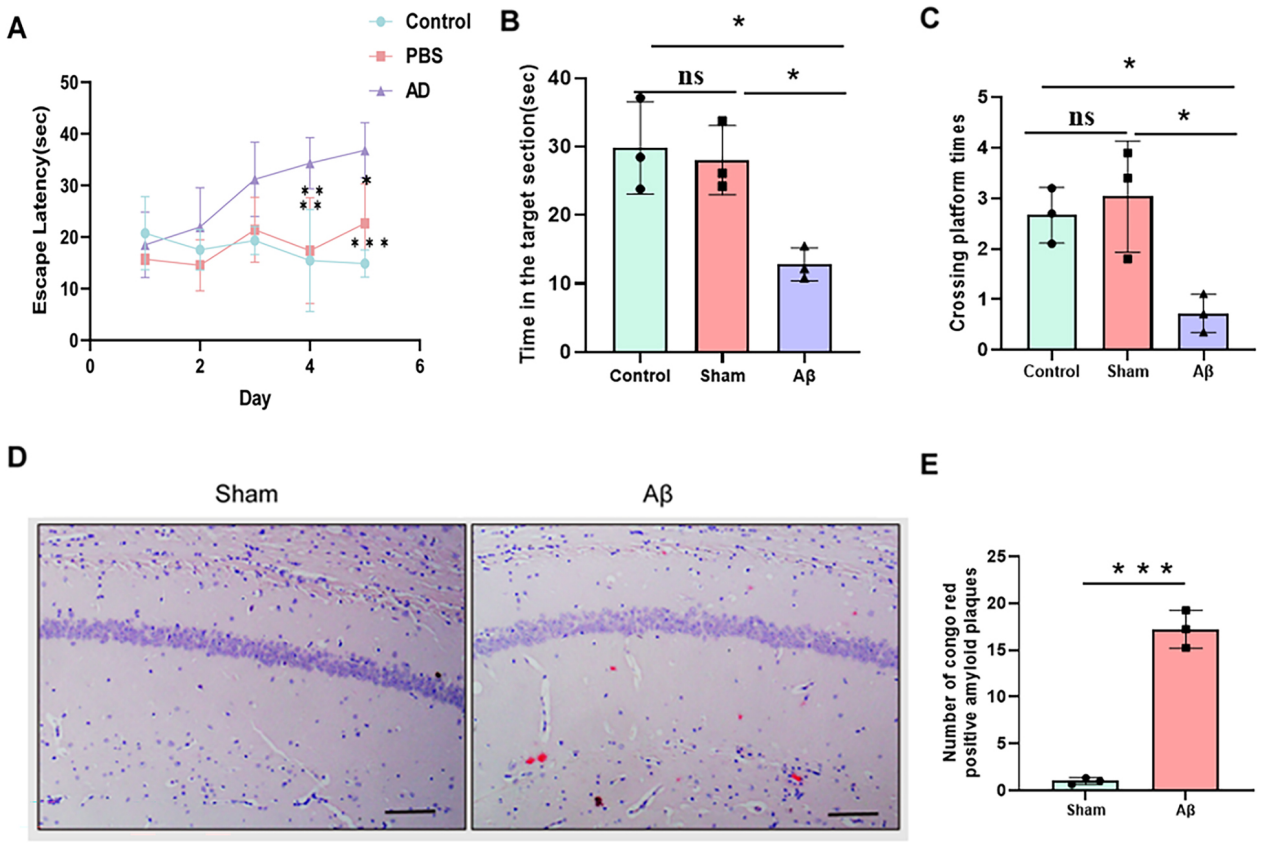

Fig. 3. AD rat model results. (A) The latency for all groups to escape in the location-navigation exam. (B,C) In the spatial probe test, the number of platform crossings and the time in the target section in each group. (D) Aβ deposition was detected in the rats' hippocampus CA1 of the sham and Aβ groups by Congo red, scale bars: 50 µm. (E) Quantitative assessment of Congo red stained plaque number in 2 groups. Data were analyzed by two-way ANOVA (A), and analyzed by one-way ANOVA (B,C,E), *$p < 0.05$, **$p < 0.01$, ***$p < 0.001$; ns, not significant, $n = 3$. Abbreviations: AD, Alzheimer's disease; CA1, cornu ammonis 1; Aβ, amyloid plaques.

3.3 Establishment of a Rat AD Model

Aβ1–42 or PBS was injected into the hippocampal CA1 region in multiple groups. Fourteen days later, three rats were randomly selected from the sham and Aβ groups for the Morris water maze test and Congo red staining. The water maze test results indicated that rats in the Aβ group wasted more time finding the platform than did those in the Sham group (Fig. 3A). In the spatial probe test, frequency of crossing the removed platform was lower (Fig. 3B), and the duration in the target quadrant was shorter for rats in the Aβ group than for those in the sham group (Fig. 3C). To eliminate the possibility that Morris water maze performance differences were confounded by motor or visual impairments, additional assessments were conducted before the formal test. These confirm that the water maze differences reflect cognitive, not motor or visual impairment. Congo red staining of the hippocampus revealed that Aβ deposition was found in the Aβ group and almost no Aβ deposition in the Sham group (Fig. 3D,E).

3.4 Transplanting HFSCs and HFSCs/NGF Improved the Cognitive and Behavioral Ability of AD Rats

To investigate the potential of transplanted HFSCs to restore behavioral deficits in AD rats, Morris water maze tests were performed 14 days post-cell transplantation. During the five-day training period, HFSC-transplanted rats exhibited a gradual increase in their ability to find a concealed platform (Fig. 4). Rats in the HFSCs/NGF transplanted group exhibited significantly better performance than did those in the HFSCs transplanted group (Fig. 4A). Throughout the spatial probe test, the frequency of crossing the eliminated platform was higher (Fig. 4B), and the duration in the target quadrant was longer in the HFSCs group and HFSCs/NGF group than in the AD group (Fig. 4C). Moreover, a significant difference in tracks of the spatial probe test on the 6th day was observed among the four groups (Fig. 4D); the rats transplanted with HFSCs and HFSCs/NGF improved their approaches for reaching the platform. In summary, these results indicated that transplantation of HFSCs and HFSCs/NGF reduced cognitive dysfunction in AD rats.

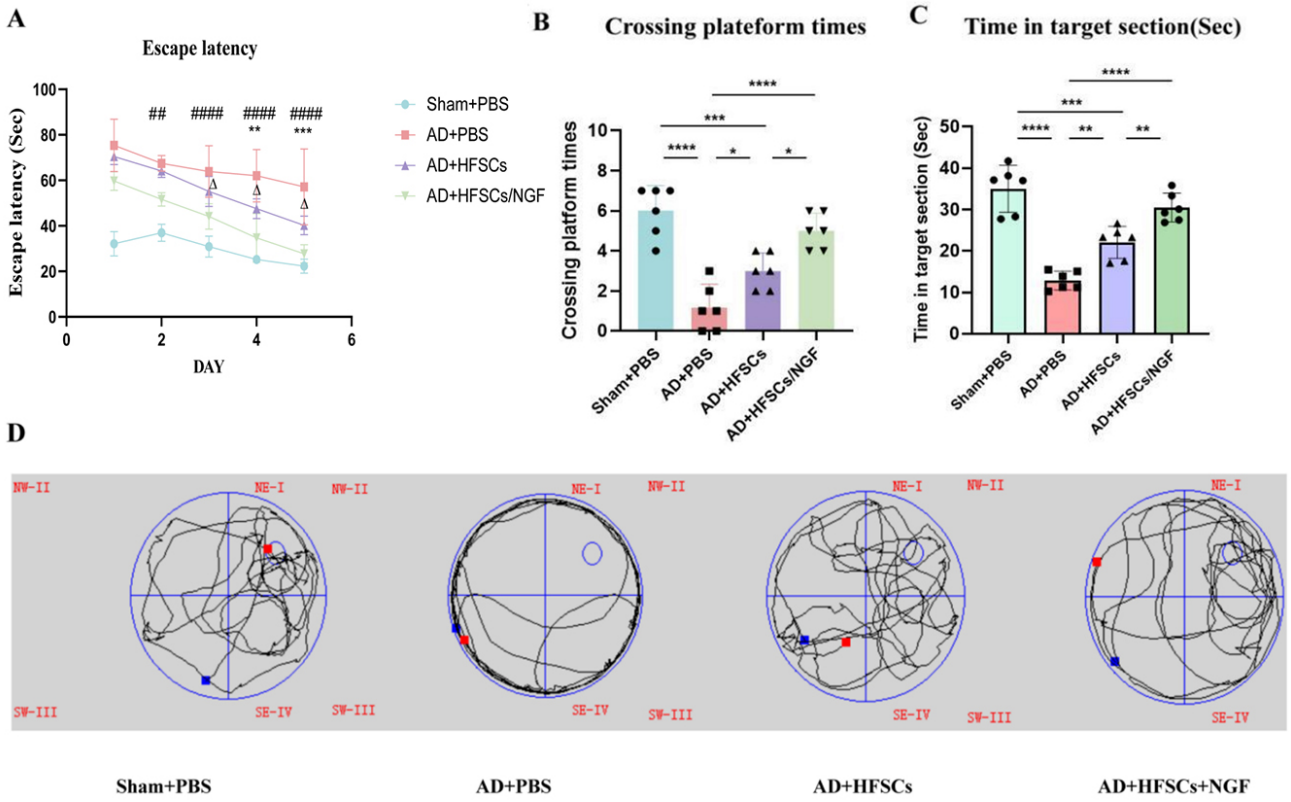

Fig. 4. HFSCs and HFSCs/NGF transplantation improved the learning and memory impairment. (A) The latency for each group to escape in the location-navigation test, in the spatial-probe test, (B) the number of platform crossing and (C) time in the target section. (D) Illustrative tracks of the spatial probe test on day 6. When comparing with the AD rats, the rats transplanted with HFSCs and HFSCs/NGF showed significantly improved learning and memory. Data were assessed by two-way ANOVA (A), and analyzed by one-way ANOVA (B,C), AD+PBS group *vs.* AD+HFSCs group, $^{*}p < 0.05$, $^{**}p < 0.01$, $^{***}p < 0.001$, $^{****}p < 0.0001$; AD+PBS group *vs.* AD+HFSCs/NGF group, $^{\#\#}p < 0.01$, $^{\#\#\#\#}p < 0.0001$; AD+HFSCs group *vs.* AD+HFSCs/NGF group, $^{\triangle}p < 0.05$, $n = 6$. Abbreviations: NW, northwest; SW, southwest; NE, northeast; SE, southeast.

3.5 HFSCs and HFSCs/NGF Transplantation Decreased Aβ Deposition

To investigate the effects of HFSCs and HFSCs/NGF transplantation on the production of toxic amyloid plaques, immunohistochemistry was conducted using 6E10 antibodies in the brains of AD rats (Fig. 5A). Quantification of stained plaques in the hippocampus revealed significant variations between the HFSCs and the HFSCs/NGF groups (Fig. 5B). Protein levels were measured in four rat groups using Aβ1–40 and Aβ1–42 ELISA kits (Fig. 5C,D). Compared to PBS-treated AD rats, levels of Aβ1–40 and Aβ1–42 had significantly declined in both the HFSCs group and HFSCs/NGF group rats, as measured by ELISA. These findings led to the conclusion that HFSCs and HFSCs/NGF transplantation in AD rats could decrease the levels of Aβ1–40 and Aβ1–42. To elucidate the mechanisms underlying the reduction of Aβ depositions in HFSCs and HFSCs/NGF group AD rats, the BACE1 levels were quantified by western blot analysis (Fig. 5E,F, the original WB images can be found in the **Supplementary Material**). The levels of BACE1 in the hippocampus of the HFSCs group and HFSCs/NGF group rats were significantly lower than those in the AD group rats. These data provide evidence that the level of BACE1 declined in the hippocampus during the HFSCs or HFSCs/NGF transplantation, thereby inhibiting the AβPP amyloid hydrolysis pathway.

3.6 HFSCs and HFSCs/NGF Transplantation Reduced Tau Hyperphosphorylation

Another important pathology of AD is tau hyperphosphorylation. To verify the consequences of HFSCs and HFSCs/NGF on tau hyperphosphorylation, the phosphorylation levels of tau 5 and other tau sites were quantified by using western blot analysis. The outcomes illustrated that HFSCs and HFSCs/NGF transplantation inhibited tau 5 and tau phosphorylation at Ser202/Thr205, Thr231, S396, and S404 sites in the AD rat hippocampus (Fig. 6, the original WB images can be found in the **Supplementary Material**).

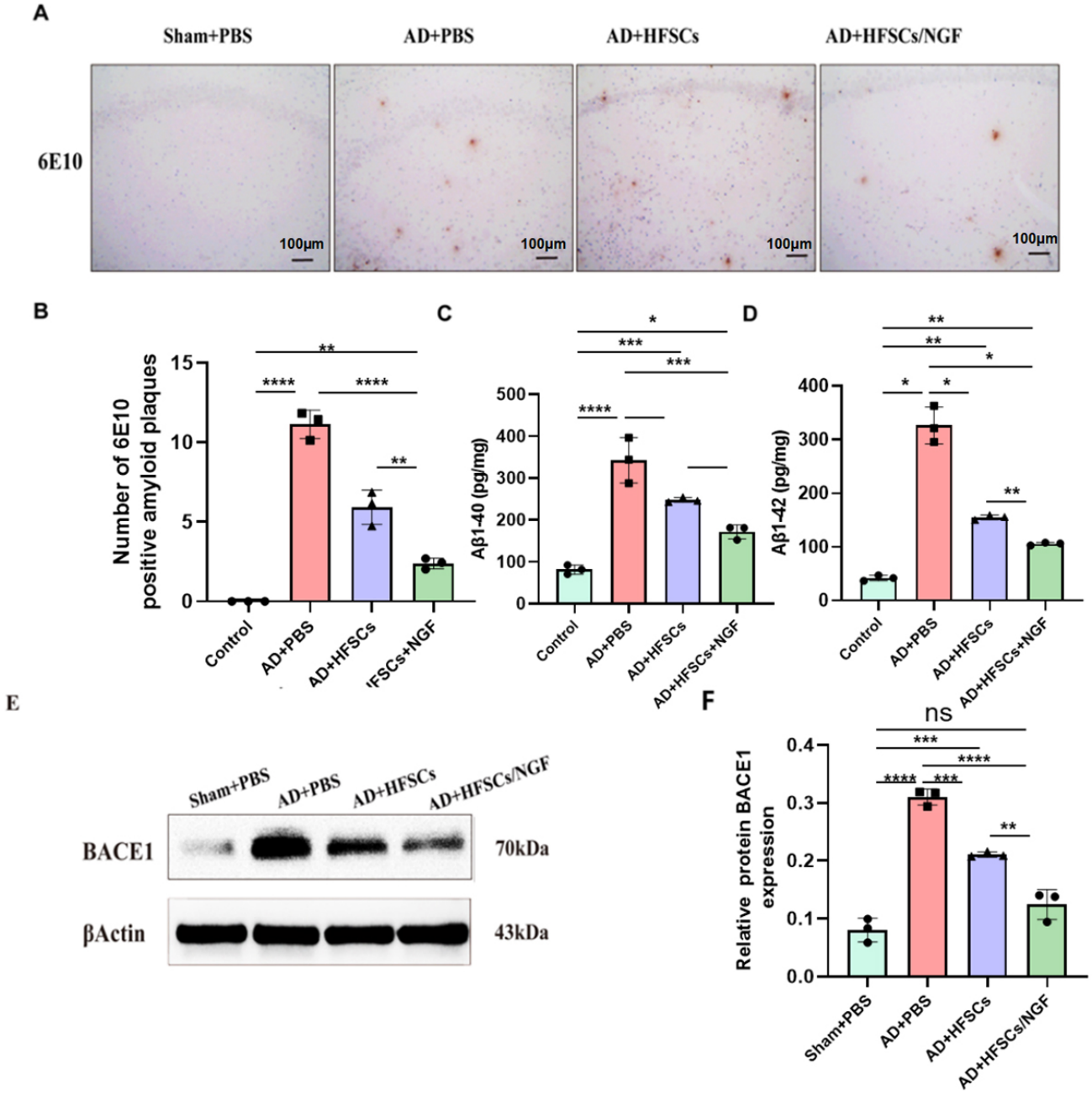

Fig. 5. HFSCs and HFSCs/NGF transplantation declined the level of Aβ40 and Aβ42. (A) Amyloid plaques were quantified by immunohistochemistry via 6E10 antibody. (B) Quantitative assessment of 6E10 stained plaque number in CA1 area. (C,D) Compared with PBS-treated AD rats, Aβ1–40 and Aβ1–42 levels were markedly decreased in HFSCs and HFSCs/NGF group rats as measured by ELISA. (E) The BACE1 protein level was assessed by western blot in the hippocampus of rats. (F) The relative quantification of BACE1 protein expression. Scale bars: 100 μm. One-way ANOVA with Tukey's post-hoc test was utilized to analyze data (B–D,F), *$p < 0.05$, **$p < 0.01$, ***$p < 0.001$, ****$p < 0.0001$; ns, not significant, $n = 3$. Abbreviations: BACE1, β-site amyloid precursor protein cleaving enzyme 1; ELISA, enzyme-linked immunosorbent assay.

3.7 HFSCs and HFSCs/NGF Transplantation Inhibited GSK-3β by Activating PI3K/Akt Signaling

Proteins of the PI3K/Akt/GSK3β pathway were examined with western blot analysis (Fig. 7, the original WB images can be found in the **Supplementary Material**), which revealed significantly higher levels of phosphorylated PI3K and phosphorylated Akt after transplantation of HFSCs and HFSCs/NGF than in both the Sham group and the AD group. Additionally, the levels of phosphorylated GSK3β at the Ser9 site to suppress GSK3β activity were significantly raised in the HFSCs and the HFSCs/NGF groups. Total PI3K, Akt, and GSK3β were investigated as

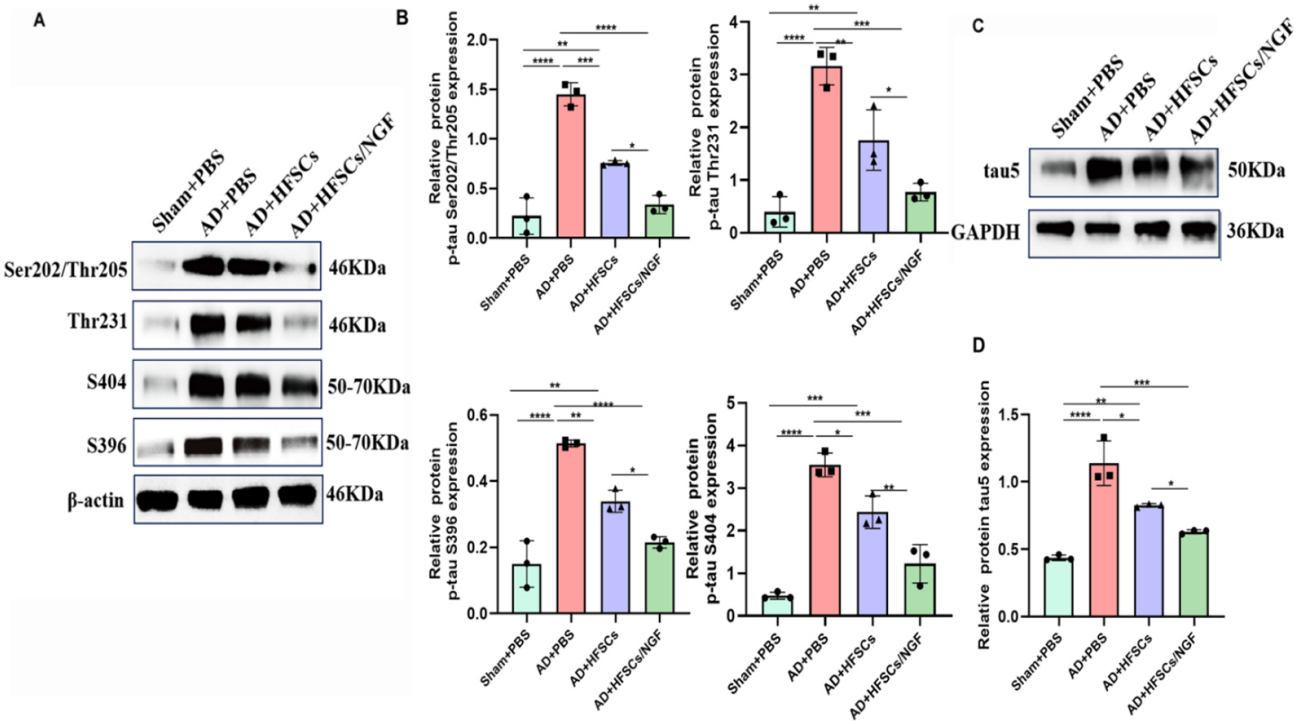

Fig. 6. HFSCs and HFSCs/NGF transplantation reduced tau hyperphosphorylation. (A) The tau phosphorylation site levels were quantified by western blot analysis, showing that HFSCs and HFSCs/NGF transplantation inhibited tau phosphorylation at Ser202/Thr205, Thr231, S396, and S404 sites in the hippocampus of AD rats. (B) The relative quantification of Ser202/Thr205, Thr231, S396, and S404 sites protein expression. (C) The tau 5 concentration was assessed by western blot analysis in the hippocampus. (D) The relative quantification of tau5 protein expression. One-way ANOVA with Tukey's post-hoc test was utilized to analyze the data (B,D), $*p < 0.05$, $**p < 0.01$, $***p < 0.001$, $****p < 0.0001$, $n = 3$. GAPDH, anti-glyceraldehyde- 3-phosphate dehydrogenase.

loading controls. These results revealed that HFSCs and HFSCs/NGF transplantation could reduce tau hyperphosphorylation by the PI3K/Akt pathway activation to suppress GSK3β activity.

3.8 HFSCs and HFSCs/NGF Transplantation Reduced Synaptic Protein Damage

Of all the pathological changes that occur in the brains of individuals with AD, synaptic loss is most strictly related to cognitive decline [34]. Therefore, we analyzed the SYP and PSD-95 levels in the hippocampus of the four groups by immunohistochemical staining and western blotting (Fig. 8). The SYP and PSD-95 levels were significantly lower in AD+PBS rats than in Sham+PBS rats. However, after HFSCs and HFSCs/NGF transplantation, the level of SYP rose significantly (Fig. 8A,B, the original WB images can be found in the **Supplementary Material**). The PSD-95 level displayed a significant elevation in the HFSCs/NGF group, but no significant difference was shown between the AD+PBS and the AD+HFSCs groups (Fig. 8C,D).

4. Discussion

AD is characterized by the presence of amyloid plaques and fibrillary tangles, along with massive neuronal death and synaptic disruption in various brain regions. Stem cell transplantation is one approach for treating AD. However, the present study is the first attempt to treat AD model rats using HFSCs. Due to advancements in genetic engineering, transplantation of transgenic stem cells overexpressing specific factors can significantly enhance the reparative potential of native stem cells. This potential restoration is attributed to several mechanisms, including improved survival and differentiation capabilities of the transplanted cells, apoptosis suppression, reduction in infarct volume, and enhancement of neovascularization or functional recovery [35]. Herein, we explored the potential mechanism of HFSCs and NGF-modified HFSCs on AD-like behaviors in an Aβ-injected rat model. The results revealed that hippocampus stereotaxic injection of HFSCs or NGF-modified HFSCs could ameliorate AD-like behaviors, as indicated by the progressive improvement of the performance of the treated rats in the Morris water maze test. Moreover, Aβ deposition and tau hyperphosphorylation in the AD rats were significantly improved after stereotaxic injection of HFSCs or NGF-modified HFSCs, with a

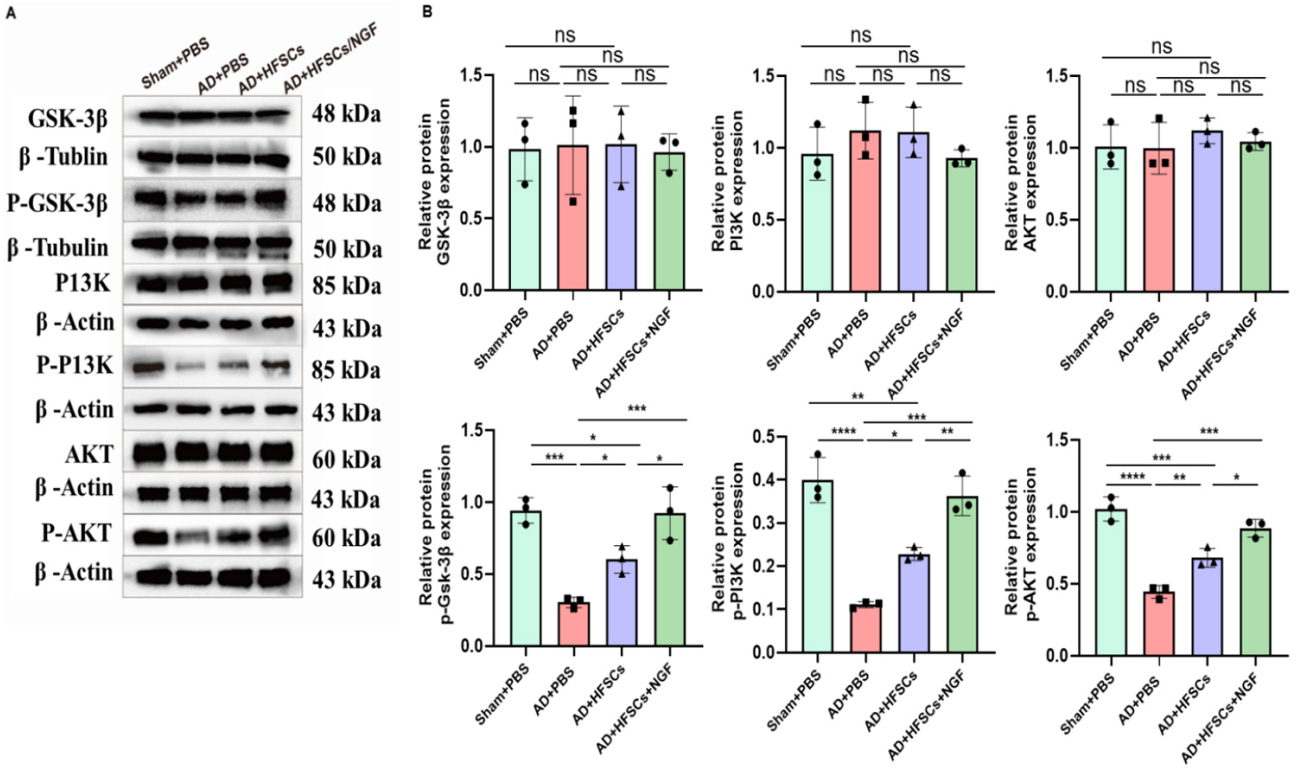

Fig. 7. HFSCs and HFSCs/NGF transplantation inhibited the activity of GSK3β through PI3K/Akt pathways activation. (A) The levels of GSK3β, p-GSK-3β, PI3K, p-PI3K, Akt, and p-Akt were quantified by immunoblots and (B) the relative quantification of protein expression in each group. One-way ANOVA with Tukey's post-hoc test was utilized to analyze data (B), *$p < 0.05$, **$p < 0.01$, ***$p < 0.001$, ****$p < 0.0001$; ns, not significant, $n = 3$. Abbreviations: GSK3β, glycogen synthase kinase 3β; PI3K, phosphoinositide-3 kinase; Akt, protein kinase B; p-PI3K, phosphorylated PI3K; p-Akt, phosphorylated Akt; p-GSK3β, phosphorylated GSK3β.

reduction in protein expression of BACE1, Aβ1–40, and Aβ1–42. These results suggested that HFSCs and NGF-modified HFSCs can improve AD-like memory deficits by activating the PI3K/Akt/GSK3β pathway.

Aβ overproduction and amyloid plaque buildup in the AD brain reduce the long-term survival of recently produced neurons and hinder adult hippocampal neurogenesis [36]. After treatment with HFSCs and NGF-modified HFSCs, levels of Aβ deposition declined significantly in the HFSCs and HFSCs/NGF groups. Moreover, the western blot results for BACE1 showed a decline in these two groups, suggesting that HFSCs and NGF-modified HFSCs inhibited the process of Aβ production. The significant suppression in Aβ1–40 and Aβ1–42 levels also demonstrated that HFSCs and HFSCs/NGF could decrease neurotoxic proteins and the resulting damage. Earlier investigations have illustrated that stem cells can enhance cognitive function in AD rats through similar mechanisms [37].

Another common pathological change associated with AD is excessive tau protein phosphorylation of NFTs in neurons. Notably, both Aβ and tau protein oligomers exhibit neural toxicity independently; their pathology is interconnected. Many investigations have found that Aβ oligomers disrupt the normal activity of wingless-related integration site (Wnt) pathways, resulting in an elevation in the activity of GSK3β [38], subsequently promoting tau phosphorylation [39]. Therefore, after HFSCs and HFSCs/NGF transplantation, we examined whether the expression of phosphorylated tau and GSK3β. GSK3β was inhibited by phosphorylation at Ser9. We found that, compared to the Sham+PBS group, there was a significant decline in phosphorylated-GSK3β in the AD+PBS group. The GSK-3β phosphorylation at Ser9 was significantly higher in HFSCs-treated AD rats than in PBS-treated AD rats, indicating an inhibitory effect on GSK-3β signaling. GSK-3β excessively phosphorylates tau at the Thr231 site, causing it to accumulate within cells. This buildup leads to the formation of NFTs and the inability of microtubules to bind and assemble properly. The accumulation of hyperphosphorylated tau disrupts synaptic function, impedes axonal transport, impacts neurotrophic function, and leads to the death of neurons by initiating apoptotic signals.

Phosphorylation of GSK3β also affects long-term memory in tasks [40]. Activated GSK-3β upregulates the NF-κB pathway to generate inflammatory factors (IL-6, TNF-α, and IL-1β) and reduces the anti-inflammatory factors, synthesis containing IL-10. This imbalance between GSK-3β-related inflammatory and anti-inflammatory re-

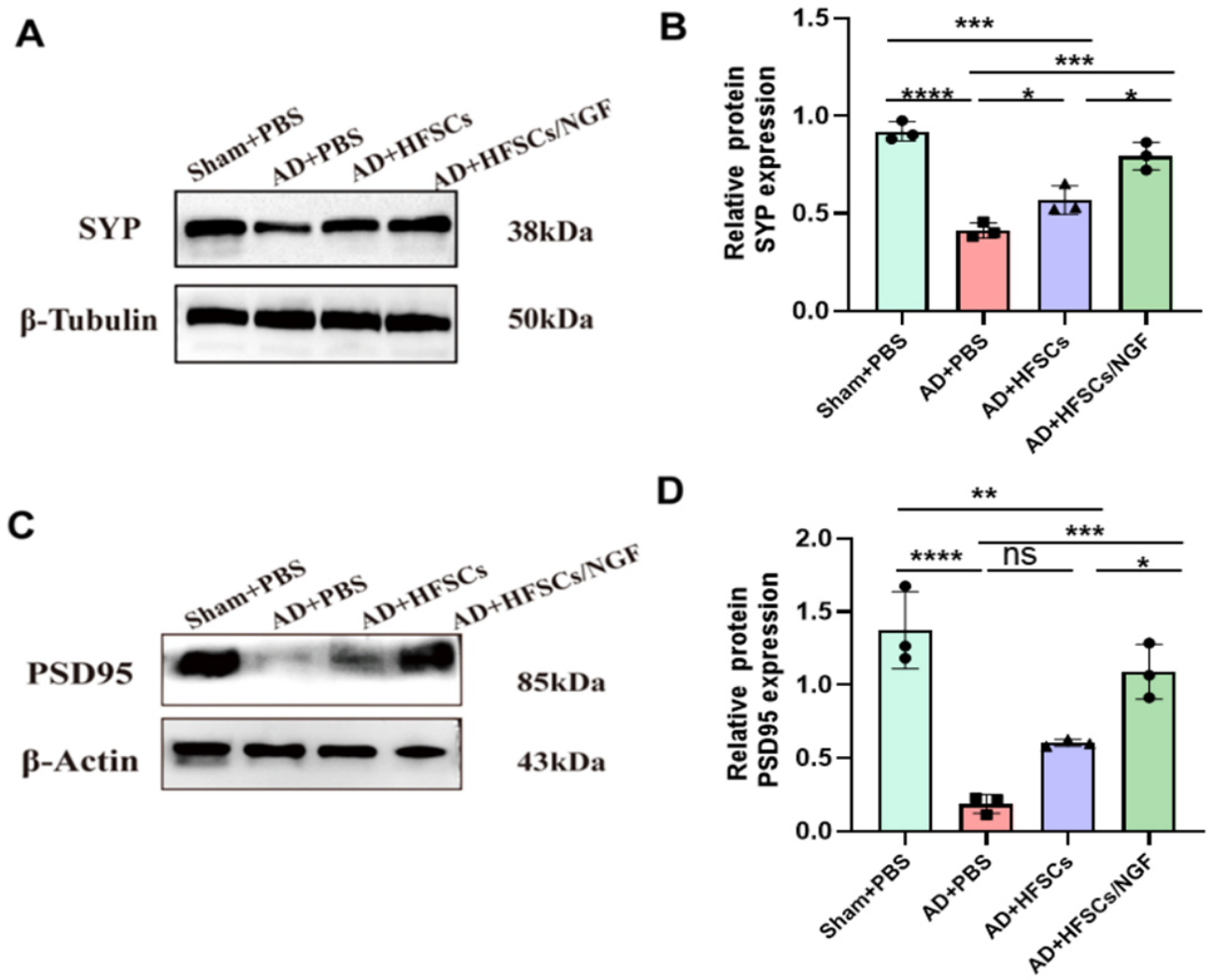

Fig. 8. HFSCs transplantation increased the level of synaptophysin and PSD-95 expression. (A) The SYP protein level was assessed by western blot analysis in the hippocampus of three groups. (B) The relative quantification of protein expression. (C) The PSD-95 protein level was assessed by western blot analysis in the hippocampus of three groups. (D) The relative quantification of protein expression. Data were analyzed by one-way ANOVA with Tukey's post-hoc test (B,D), *$p < 0.05$, **$p < 0.01$, ***$p < 0.001$, ****$p < 0.0001$; ns, not significant, $n = 3$. Abbreviations: PSD-95, postsynaptic density-95; SYP, synaptophysin.

sults continues to exacerbate the pathological processes. Activation of GSK-3β exerts a detrimental effect on mitochondrial function, elevating the expression of caspase-3 and caspase-9 and ultimately inducing neuronal apoptosis. Conversely, inhibiting GSK-3β lowers the production of caspase and caspase cytokines, which helps to prevent neuronal apoptosis [41]. Therefore, the effects of HFSCs and HFSCs/NGF on reducing AD-like manifestations are closely linked to the suppression of GSK-3β activity.

Synaptic proteins are crucial molecules that constitute the synaptic structure and are closely related to neurotransmitter secretion and synaptic plasticity [42]. Therefore, the expression levels of synaptic proteins can serve as molecular markers of synaptic plasticity, particularly long-term-potentiation capacity. Synaptic proteins include presynaptic and postsynaptic-membrane proteins. A study has shown that soluble Aβ and tau proteins have a direct toxic effect on synapses, which can damage synaptic proteins and result in cognitive deficits [43]. Our results were in line with reports that mesenchymal stem cell transplantation into the brains of AD rats reduces synapse-related protein damage and alleviates cognitive impairment [44,45]. The beneficial effects of HFSCs and NGF/HFSCs on synaptic protein damage in AD rats might be mediated by two mechanisms. The first mechanism might involve the reduction of excessive phosphorylation of soluble Aβ and tau within the brain, reducing their detrimental effects on synapse proteins and ameliorating long-term-potentiation impairment. The second mechanism might involve the HFSCs' amelioration of synaptic plasticity and cognitive dysfunction by activating the PI3K/Akt/Wnt/beta-catenin pathway [46].

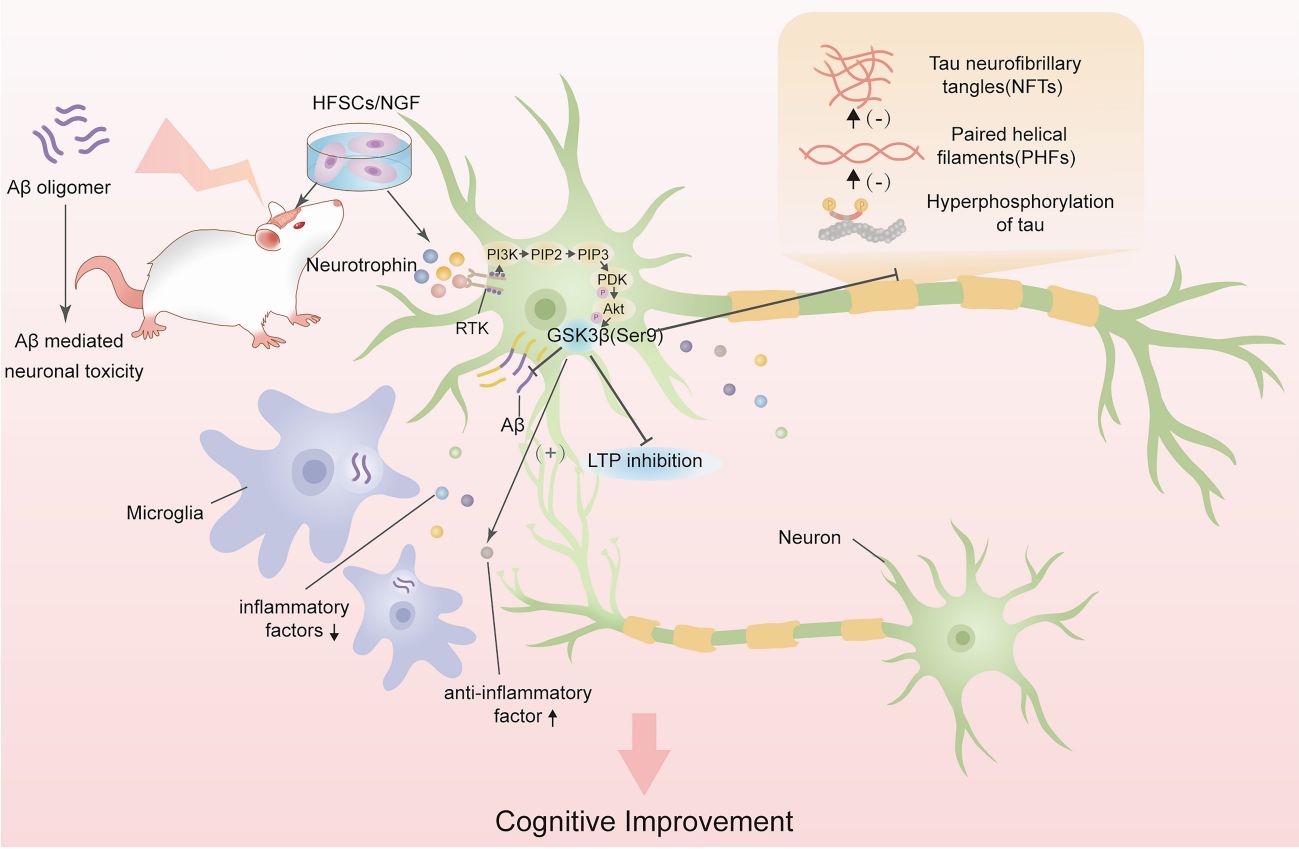

Fig. 9. Overview diagram of the mechanism of HFSCs and HFSCs/NGF treatment in AD rats. Dots: Signaling molecules (e.g., neurotrophic/inflammatory factors). Arrows: Regulatory direction; "↑"/"↓": Substance upregulation/downregulation; "(+)"/"(-)": Biological effect enhancement/inhibition. Abbreviations: Aβ, Amyloid-β; RTK, receptor tyrosine kinase; LTP, long-term potentiation; NFTs, neurofibrillary tangles; PHFs, paired helical filaments.

NGF is necessary for neuronal growth, survival, inhibition of apoptosis, supporting stem cell survival, multiplication, differentiation, and enhancing memory in AD rat models [47]. Furthermore, PI3K is important for NGF-stimulated TrkA internalization [27]. Owing to NGF stimulation, the PI3K/Akt pathway participates in enhancing cholinergic gene expression, neurite elongation [48], and cell survival [49]. The activated Akt enzyme phosphorylates and inhibits its downstream target, GSK3β, leading to a mitigated accumulation of hyperphosphorylated tau protein [50]. Moreover, exogenous NGF administered to cholinergic neurons in the basal forebrain counteracted the reduced retrograde transport of NGF, thereby reducing the synthesis and expression of amyloid precursor proteins, alleviating cholinergic neuron degeneration, and inhibiting the hyperphosphorylation of tau [41]. NGF possesses a crucial function in the PI3K/Akt signaling pathway by indirectly influencing transcription factors, including calcium/calcineurin-dependent nuclear factor of activated T cells (NFAT). Activating NFAT is critical for synaptic plasticity during development [51] and is attributed to synaptotoxicity in AD [52,53]. Through the Akt/GSK3β/NFAT pathway, NGF also prevents mitochondria-mediated apoptosis-induced cytotoxicity by inhibiting GSK3β and preserving NFAT expression levels [54]. Conversely, NFAT can promote neurite outgrowth triggered by NGF [54]. These mechanisms are important for treating AD.

HFSCs have drawn much attention because of their convenient accessibility, strong proliferation, and wide-ranging potential for differentiation [55,56]. Consequently, they have excellent neural differentiation and neurotrophic abilities [18,57]. In spinal-cord-injury rat models, transplanted HFSCs survive and proliferate within the injured rat spinal cord. These cells can differentiate into glial cell lineages (including astrocytes and oligodendrocytes) and neurons. Oligodendrocytes contribute to myelin repair around intact and demyelinated axons. Furthermore, hair-follicle stem cells express neurotrophic factors and other nutritional substances that collectively facilitate nerve repair and promote functional recovery [58]. In rats with ischemic stroke, transplantation of HFSCs significantly inhibited the activation of microglia to suppress inflammatory responses, enhanced the integrity of the blood-brain barrier, and reduced cerebral edema [59].

Recent investigations have indicated that HFSCs could secrete various neuroprotective agents [60], which may explain the progressive improvement in the performance of rats treated with HFSCs. Moreover, Tang [59] has shown that HFSCs could regulate astrocyte stimulation through paracrine cytokines (transforming growth factor-β (TGF-β) and IL-4). Neuroinflammation is widely recognized to have an essential involvement in AD [61–64]. Microglial cells and astrocytes are frequently activated in the CNS in neurodegenerative diseases. Therefore, we will elucidate the effect of transplanted HFSCs on the neuroinflammation of AD rats in further studies.

Overall, our data have indicated that HFSCs and NGF/HFSCs injections are a promising therapy for restoring the behavioral decline that is a characteristic symptom of AD. Our research results supported the concept that neuroprotection of HFSCs and NGF/HFSCs is exerted by their capacity to reduce Aβ deposition, tau hyperphosphorylation and synaptic protein injury (Fig. 9). In addition, HFSCs overexpressing NGF displayed a greater ability to ameliorate cognitive dysfunction in AD rats than did HFSCs alone. Each adult has over five million hair follicles, which are a common skin appendage and a plentiful and convenient source of HFSCs, making them an excellent option for stem cell therapy for AD [56].

Although our investigation offers proof for the application of HFSCs in the therapy of AD rats, we acknowledge that further research about HFSCs in the treatment of AD is necessary. The present study had some limitations, including the need to clarify the *in vivo* expression, localization, and differentiation of NGF-overexpressing HFSCs in the brain; the need to evaluate the neuroinflammatory response induced during Aβ modeling; and the need to set up a NGF-free protein control group, to rule out confounding factors such as the dilution effect of transplanted cells that may interfere with the results. These limitations will serve as important guides for our subsequent research, prompting us to conduct more in-depth investigations into the therapeutic value and underlying mechanisms of HFSCs in AD, thereby enhancing the robustness and translational relevance of our findings.

5. Conclusions

In this study, we discovered a new therapeutic effect of HFSCs that could serve as a new treatment for AD. The utilization of HFSCs decreased Aβ deposition and tau hyperphosphorylation in AD rats, with the therapeutic effect being mediated through activating PI3K/Akt signaling. Moreover, the combination of HFSCs and NGF was verified to be more effective than translated HFSCs alone in the AD model. Overall, HFSCs and NGF-modified HFSCs show significant promise as a viable and secure therapeutic approach for AD, with the possibility for future use in clinical settings.

Availability of Data and Materials

The datasets generated during the current study are available from the corresponding authors upon reasonable requests.

Author Contributions

DY and LL: conception and design, experiments execution, collection and assembly of data, data analysis and interpretation, manuscript writing; JF: conception and design, supervised the study, revised the manuscript. All authors read and approved the final manuscript. All authors have participated sufficiently in the work and agreed to be accountable for all aspects of the work.

Ethics Approval and Consent to Participate

All animal experiments were conducted in strict adherence to the principles outlined in the "Guide for the Care and Use of Laboratory Animals" published by the Ministry of Science and Technology of the People's Republic of China. The experiment was approved by the Ethics Committee of the Second Affiliated Hospital of Harbin Medical University, with the approval number: SYDW2022-078.

Acknowledgment

We would like to thank Dr. Haitong Dou from the department of Neurology, The Second Affiliated Hospital of Harbin Medical University, for her guidance in cultivating cells.

Funding

This research received no external funding.

Conflict of Interest

The authors declare no conflict of interest.

Supplementary Material

Supplementary material associated with this article can be found, in the online version, at https://doi.org/10.31083/JIN43410.

References

[1] Scheltens P, De Strooper B, Kivipelto M, Holstege H, Chételat G, Teunissen CE, *et al*. Alzheimer's disease. Lancet. 2021; 397: 1577–1590. https://doi.org/10.1016/S0140-6736(20)32205-4.

[2] Comas-Herrera A, Guerchet M, Karagiannidou M, Knapp M, Prince M. World Alzheimer Report 2016: Improving healthcare for people living with dementia: Coverage, quality and costs now and in the future. 2016. Available at: https://www.alzint.org/resource/world-alzheimer-report-2016/ (Accessed: 21 September 2016).

[3] World Health Organization. Dementia. 2021. Available at: https://www.who.int/news-room/facts-in-pictures/detail/dementia (Accessed: 8 August 2024).

[4] Huang LK, Chao SP, Hu CJ. Clinical trials of new drugs for Alzheimer disease. Journal of Biomedical Science. 2020; 27: 18. https://doi.org/10.1186/s12929-019-0609-7.

[5] National Center for Health Statistics. Health, United States - Data Finder. 2024. Available at: https://www.cdc.gov/nchs/hus/data-finder.htm (Accessed: 8 August 2024).
[6] Jeong S. Molecular and Cellular Basis of Neurodegeneration in Alzheimer's Disease. Molecules and Cells. 2017; 40: 613–620. https://doi.org/10.14348/molcells.2017.0096.
[7] Zhou F, Zhao Y, Sun Y, Chen W. Molecular Insights into Tau Pathology and Its Therapeutic Strategies in Alzheimer's Disease. Journal of Integrative Neuroscience. 2024; 23: 197. https://doi.org/10.31083/j.jin2311197.
[8] De Strooper B, Karran E. The Cellular Phase of Alzheimer's Disease. Cell. 2016; 164: 603–615. https://doi.org/10.1016/j.cell.2015.12.056.
[9] Howard R, McShane R, Lindesay J, Ritchie C, Baldwin A, Barber R, *et al*. Donepezil and memantine for moderate-to-severe Alzheimer's disease. The New England Journal of Medicine. 2012; 366: 893–903. https://doi.org/10.1056/NEJMoa1106668.
[10] Grossberg GT, Manes F, Allegri RF, Gutiérrez-Robledo LM, Gloger S, Xie L, *et al*. The safety, tolerability, and efficacy of once-daily memantine (28 mg): a multinational, randomized, double-blind, placebo-controlled trial in patients with moderate-to-severe Alzheimer's disease taking cholinesterase inhibitors. CNS Drugs. 2013; 27: 469–478. https://doi.org/10.1007/s40263-013-0077-7.
[11] Larkin HD. Lecanemab gains FDA approval for early Alzheimer disease. JAMA. 2023; 329: 363. https://doi.org/10.1001/jama.2022.24490.
[12] Wei L, Wei ZZ, Jiang MQ, Mohamad O, Yu SP. Stem cell transplantation therapy for multifaceted therapeutic benefits after stroke. Progress in Neurobiology. 2017; 157: 49–78. https://doi.org/10.1016/j.pneurobio.2017.03.003.
[13] De Gioia R, Biella F, Citterio G, Rizzo F, Abati E, Nizzardo M, *et al*. Neural Stem Cell Transplantation for Neurodegenerative Diseases. International Journal of Molecular Sciences. 2020; 21: 3103. https://doi.org/10.3390/ijms21093103.
[14] Giusto E, Donegà M, Cossetti C, Pluchino S. Neuro-immune interactions of neural stem cell transplants: from animal disease models to human trials. Experimental Neurology. 2014; 260: 19–32. https://doi.org/10.1016/j.expneurol.2013.03.009.
[15] Amoh Y, Li L, Katsuoka K, Penman S, Hoffman RM. Multipotent nestin-positive, keratin-negative hair-follicle bulge stem cells can form neurons. Proceedings of the National Academy of Sciences of the United States of America. 2005; 102: 5530–5534. https://doi.org/10.1073/pnas.0501263102.
[16] McKenzie IA, Biernaskie J, Toma JG, Midha R, Miller FD. Skin-derived precursors generate myelinating Schwann cells for the injured and dysmyelinated nervous system. The Journal of Neuroscience. 2006; 26: 6651–6660. https://doi.org/10.1523/JNEUROSCI.1007-06.2006.
[17] Belicchi M, Pisati F, Lopa R, Porretti L, Fortunato F, Sironi M, *et al*. Human skin-derived stem cells migrate throughout forebrain and differentiate into astrocytes after injection into adult mouse brain. Journal of Neuroscience Research. 2004; 77: 475–486. https://doi.org/10.1002/jnr.20151.
[18] Li M, Liu JY, Wang S, Xu H, Cui L, Lv S, *et al*. Multipotent neural crest stem cell-like cells from rat vibrissa dermal papilla induce neuronal differentiation of PC12 cells. BioMed Research International. 2014; 2014: 186239. https://doi.org/10.1155/2014/186239.
[19] Shih DTB, Lee DC, Chen SC, Tsai RY, Huang CT, Tsai CC, *et al*. Isolation and characterization of neurogenic mesenchymal stem cells in human scalp tissue. Stem Cells. 2005; 23: 1012–1020. https://doi.org/10.1634/stemcells.2004-0125.
[20] Levi-Montalcini R. The nerve growth factor 35 years later. Science. 1987; 237: 1154–1162. https://doi.org/10.1126/science.3306916.
[21] Aloe L, Rocco ML, Bianchi P, Manni L. Nerve growth factor: from the early discoveries to the potential clinical use. Journal of Translational Medicine. 2012; 10: 239. https://doi.org/10.1186/1479-5876-10-239.
[22] Biane J, Conner JM, Tuszynski MH. Nerve growth factor is primarily produced by GABAergic neurons of the adult rat cortex. Frontiers in Cellular Neuroscience. 2014; 8: 220. https://doi.org/10.3389/fncel.2014.00220.
[23] Madziar B, Lopez-Coviella I, Zemelko V, Berse B. Regulation of cholinergic gene expression by nerve growth factor depends on the phosphatidylinositol-3'-kinase pathway. Journal of Neurochemistry. 2005; 92: 767–779. https://doi.org/10.1111/j.1471-4159.2004.02908.x.
[24] Higuchi M, Onishi K, Masuyama N, Gotoh Y. The phosphatidylinositol-3 kinase (PI3K)-Akt pathway suppresses neurite branch formation in NGF-treated PC12 cells. Genes to Cells. 2003; 8: 657–669. https://doi.org/10.1046/j.1365-2443.2003.00663.x.
[25] Fiore M, Mancinelli R, Aloe L, Laviola G, Sornelli F, Vitali M, *et al*. Hepatocyte growth factor, vascular endothelial growth factor, glial cell-derived neurotrophic factor and nerve growth factor are differentially affected by early chronic ethanol or red wine intake. Toxicology Letters. 2009; 188: 208–213. https://doi.org/10.1016/j.toxlet.2009.04.013.
[26] Klesse LJ, Parada LF. Trks: signal transduction and intracellular pathways. Microscopy Research and Technique. 1999; 45: 210–216. https://doi.org/10.1002/(SICI)1097-0029(19990515/01)45:4/5<210::AID-JEMT4>3.0.CO;2-F.
[27] York RD, Molliver DC, Grewal SS, Stenberg PE, McCleskey EW, Stork PJ. Role of phosphoinositide 3-kinase and endocytosis in nerve growth factor-induced extracellular signal-regulated kinase activation via Ras and Rap1. Molecular and Cellular Biology. 2000; 20: 8069–8083. https://doi.org/10.1128/MCB.20.21.8069-8083.2000.
[28] Chao MV, Rajagopal R, Lee FS. Neurotrophin signalling in health and disease. Clinical Science. 2006; 110: 167–173. https://doi.org/10.1042/CS20050163.
[29] Marlin MC, Li G. Biogenesis and function of the NGF/TrkA signaling endosome. International Review of Cell and Molecular Biology. 2015; 314: 239–257. https://doi.org/10.1016/bs.ircmb.2014.10.002.
[30] Matsumoto K, Sato C, Naka Y, Whitby R, Shimizu N. Stimulation of neuronal neurite outgrowth using functionalized carbon nanotubes. Nanotechnology. 2010; 21: 115101. https://doi.org/10.1088/0957-4484/21/11/115101.
[31] Reichardt LF. Neurotrophin-regulated signalling pathways. Philosophical Transactions of the Royal Society B: Biological Sciences. 2006; 361: 1545–1564. https://doi.org/10.1098/rstb.2006.1894.
[32] Song K, Huang M, Shi Q, Du T, Cao Y. Cultivation and identification of rat bone marrow-derived mesenchymal stem cells. Molecular Medicine Reports. 2014; 10: 755–760. https://doi.org/10.3892/mmr.2014.2264.
[33] Zhang XM, Ouyang YJ, Yu BQ, Li W, Yu MY, Li JY, *et al*. Therapeutic potential of dental pulp stem cell transplantation in a rat model of Alzheimer's disease. Neural Regeneration Research. 2021; 16: 893–898. https://doi.org/10.4103/1673-5374.297088.
[34] Pickett EK, Henstridge CM, Allison E, Pitstick R, Pooler A, Wegmann S, *et al*. Spread of tau down neural circuits precedes synapse and neuronal loss in the rTgTauEC mouse model of early Alzheimer's disease. Synapse. 2017; 71: e21965. https://doi.org/10.1002/syn.21965.
[35] Salehi MS, Safari A, Pandamooz S, Jurek B, Hooshmandi E, Owjfard M, *et al*. The Beneficial Potential of Genetically Modified Stem Cells in the Treatment of Stroke: a Review. Stem Cell Reviews and Reports. 2022; 18: 412–440. https://doi.org/

10.1007/s12015-021-10175-1.
[36] Kim TA, Syty MD, Wu K, Ge S. Adult hippocampal neurogenesis and its impairment in Alzheimer's disease. Zoological Research. 2022; 43: 481–496. https://doi.org/10.24272/j.issn.2095-8137.2021.479.
[37] Lee JK, Jin HK, Endo S, Schuchman EH, Carter JE, Bae JS. Intracerebral transplantation of bone marrow-derived mesenchymal stem cells reduces amyloid-beta deposition and rescues memory deficits in Alzheimer's disease mice by modulation of immune responses. Stem Cells. 2010; 28: 329–343. https://doi.org/10.1002/stem.277.
[38] Magdesian MH, Carvalho MMVF, Mendes FA, Saraiva LM, Juliano MA, Juliano L, *et al*. Amyloid-beta binds to the extracellular cysteine-rich domain of Frizzled and inhibits Wnt/beta-catenin signaling. The Journal of Biological Chemistry. 2008; 283: 9359–9368. https://doi.org/10.1074/jbc.M707108200.
[39] Hernández F, Gómez de Barreda E, Fuster-Matanzo A, Lucas JJ, Avila J. GSK3: a possible link between beta amyloid peptide and tau protein. Experimental Neurology. 2010; 223: 322–325. https://doi.org/10.1016/j.expneurol.2009.09.011.
[40] Lauretti E, Dincer O, Praticò D. Glycogen synthase kinase-3 signaling in Alzheimer's disease. Biochimica et Biophysica Acta. Molecular Cell Research. 2020; 1867: 118664. https://doi.org/10.1016/j.bbamcr.2020.118664.
[41] Yang L, Wang H, Liu L, Xie A. The Role of Insulin/IGF-1/PI3K/Akt/GSK3β Signaling in Parkinson's Disease Dementia. Frontiers in Neuroscience. 2018; 12: 73. https://doi.org/10.3389/fnins.2018.00073.
[42] Magee JC, Grienberger C. Synaptic Plasticity Forms and Functions. Annual Review of Neuroscience. 2020; 43: 95–117. https://doi.org/10.1146/annurev-neuro-090919-022842.
[43] Hong W, Wang Z, Liu W, O'Malley TT, Jin M, Willem M, *et al*. Diffusible, highly bioactive oligomers represent a critical minority of soluble Aβ in Alzheimer's disease brain. Acta Neuropathologica. 2018; 136: 19–40. https://doi.org/10.1007/s00401-018-1846-7.
[44] Li A, Zhao J, Fan C, Zhu L, Huang C, Li Q, *et al*. Delivery of exogenous proteins by mesenchymal stem cells attenuates early memory deficits in a murine model of Alzheimer's disease. Neurobiology of Aging. 2020; 86: 81–91. https://doi.org/10.1016/j.neurobiolaging.2019.10.012.
[45] Zappa Villar MF, López Hanotte J, Pardo J, Morel GR, Mazzolini G, García MG, *et al*. Mesenchymal Stem Cells Therapy Improved the Streptozotocin-Induced Behavioral and Hippocampal Impairment in Rats. Molecular Neurobiology. 2020; 57: 600–615. https://doi.org/10.1007/s12035-019-01729-z.
[46] Hu Y, Chen W, Wu L, Jiang L, Liang N, Tan L, *et al*. TGF-β1 Restores Hippocampal Synaptic Plasticity and Memory in Alzheimer Model via the PI3K/Akt/Wnt/β-Catenin Signaling Pathway. Journal of Molecular Neuroscience. 2019; 67: 142–149. https://doi.org/10.1007/s12031-018-1219-7.
[47] Marei HES, Farag A, Althani A, Afifi N, Abd-Elmaksoud A, Lashen S, *et al*. Human olfactory bulb neural stem cells expressing hNGF restore cognitive deficit in Alzheimer's disease rat model. Journal of Cellular Physiology. 2015; 230: 116–130. https://doi.org/10.1002/jcp.24688.
[48] Wang N, Yang Y, Pang M, Du C, Chen Y, Li S, *et al*. MicroRNA-135a-5p Promotes the Functional Recovery of Spinal Cord Injury by Targeting SP1 and ROCK. Molecular Therapy Nucleic Acids. 2020; 22: 1063–1077. https://doi.org/10.1016/j.omtn.2020.08.035.
[49] Romorini L, Garate X, Neiman G, Luzzani C, Furmento VA, Guberman AS, *et al*. AKT/GSK3β signaling pathway is critically involved in human pluripotent stem cell survival. Scientific Reports. 2016; 6: 35660. https://doi.org/10.1038/srep35660.
[50] Llorens-Martín M, Jurado J, Hernández F, Avila J. GSK-3β, a pivotal kinase in Alzheimer disease. Frontiers in Molecular Neuroscience. 2014; 7: 46. https://doi.org/10.3389/fnmol.2014.00046.
[51] Nguyen T, Di Giovanni S. NFAT signaling in neural development and axon growth. International Journal of Developmental Neuroscience. 2008; 26: 141–145. https://doi.org/10.1016/j.ijdevneu.2007.10.004.
[52] Abdul HM, Sama MA, Furman JL, Mathis DM, Beckett TL, Weidner AM, *et al*. Cognitive decline in Alzheimer's disease is associated with selective changes in calcineurin/NFAT signaling. The Journal of Neuroscience. 2009; 29: 12957–12969. https://doi.org/10.1523/JNEUROSCI.1064-09.2009.
[53] Hudry E, Wu HY, Arbel-Ornath M, Hashimoto T, Matsouaka R, Fan Z, *et al*. Inhibition of the NFAT pathway alleviates amyloid β neurotoxicity in a mouse model of Alzheimer's disease. The Journal of Neuroscience. 2012; 32: 3176–3192. https://doi.org/10.1523/JNEUROSCI.6439-11.2012.
[54] Tan Z, Kang T, Zhang X, Tong Y, Chen S. Nerve growth factor prevents arsenic-induced toxicity in PC12 cells through the AKT/GSK-3β/NFAT pathway. Journal of Cellular Physiology. 2019; 234: 4726–4738. https://doi.org/10.1002/jcp.27255.
[55] Yi R. Concise Review: Mechanisms of Quiescent Hair Follicle Stem Cell Regulation. Stem Cells. 2017; 35: 2323–2330. https://doi.org/10.1002/stem.2696.
[56] Zaki AKA, Almundarij TI, Abo-Aziza FAM. Comparative characterization and osteogenic / adipogenic differentiation of mesenchymal stem cells derived from male rat hair follicles and bone marrow. Cell Regeneration. 2020; 9: 13. https://doi.org/10.1186/s13619-020-00051-7.
[57] Yang Z, Ma S, Cao R, Liu L, Cao C, Shen Z, *et al*. CD49f^{high} Defines a Distinct Skin Mesenchymal Stem Cell Population Capable of Hair Follicle Epithelial Cell Maintenance. The Journal of Investigative Dermatology. 2020; 140: 544–555.e9. https://doi.org/10.1016/j.jid.2019.08.442.
[58] Sieber-Blum M. Epidermal neural crest stem cells and their use in mouse models of spinal cord injury. Brain Research Bulletin. 2010; 83: 189–193. https://doi.org/10.1016/j.brainresbull.2010.07.002.
[59] Tang H, Zhang X, Hao X, Dou H, Zou C, Zhou Y, *et al*. Hepatocyte growth factor-modified hair follicle stem cells ameliorate cerebral ischemia/reperfusion injury in rats. Stem Cell Research & Therapy. 2023; 14: 25. https://doi.org/10.1186/s13287-023-03251-5.
[60] Chen Z, Wang Y, Shi C. Therapeutic Implications of Newly Identified Stem Cell Populations From the Skin Dermis. Cell Transplantation. 2015; 24: 1405–1422. https://doi.org/10.3727/096368914X682431.
[61] Dhapola R, Hota SS, Sarma P, Bhattacharyya A, Medhi B, Reddy DH. Recent advances in molecular pathways and therapeutic implications targeting neuroinflammation for Alzheimer's disease. Inflammopharmacology. 2021; 29: 1669–1681. https://doi.org/10.1007/s10787-021-00889-6.
[62] Heneka MT, Carson MJ, El Khoury J, Landreth GE, Brosseron F, Feinstein DL, *et al*. Neuroinflammation in Alzheimer's disease. The Lancet Neurology. 2015; 14: 388–405. https://doi.org/10.1016/S1474-4422(15)70016-5.
[63] Singh D. Astrocytic and microglial cells as the modulators of neuroinflammation in Alzheimer's disease. Journal of Neuroinflammation. 2022; 19: 206. https://doi.org/10.1186/s12974-022-02565-0.
[64] Spangenberg EE, Green KN. Inflammation in Alzheimer's disease: Lessons learned from microglia-depletion models. Brain, Behavior, and Immunity. 2017; 61: 1–11. https://doi.org/10.1016/j.bbi.2016.07.003.